Journal of Geodesy (1996) 71: 21–34

Journal of Geodesy

Downward continuation of Helmert's gravity

P. Vaníček[1], W. Sun[1,*], P. Ong[1], Z. Martinec[2], M. Najafi[1], P. Vajda[1], B. ter Horst[3]

[1]Department of Geodesy and Geomatics Engineering, University of New Brunswick, Box 4400 Frederiction, N.B. Canada E3B 5A3
[2]Department of Geophysics, Charles University, Prague, Czech Republic
[3]Faculty of Geodesy, Delft Technical University, Delft, The Netherlands
[*]*Present address*: Department of Geodesy and Photogrammetry, Royal Institute of Technology, S-100 44 Stockholm, Sweden

Received 27 October 1995; Accepted 9 July 1996

Abstract. The aim of this contribution is to show that mean Helmert's gravity anomalies obtained at the earth surface on a grid of a 'reasonable' step can be transferred to corresponding mean Helmert's anomalies on the geoid. To demonstrate this, we take the 5′ by 5′ mean Helmert's anomalies from a very rugged region, the south-western corner of Canada which contains the two main chains of the Canadian Rocky Mountains, and formulate the problem of downward continuation of Helmert's anomalies for this region. This can be done exactly because Helmert's disturbing potential is harmonic everywhere outside the geoid, therefore even within the topography. Then we solve the problem numerically by transforming the Poisson integral to a system of 53,856 linear algebraic equations. Since the matrix of this system is well conditioned, there is no theoretical obstacle to the solution. The correctness of the solution is then checked by back substitution and by evaluating the contribution of the downward continuation term to Helmert's co-geoid. This contribution comes out positive for all the points. We thus claim that the determination of the downward continuation of mean Helmert's gravity anomalies on a grid of a 'reasonable' step is a well posed problem with a unique solution and can be done routinely to any accuracy desired in the geoid computaion.

1. Introduction

In the standard Stokes formulation of the geodetic boundary value problem, the solution (the disturbing potential T) is sought above the boundary, the geoid, while the observations (gravity values g) are available on the surface of the earth (Heiskanen and Moritz, 1967). To obtain the boundary values, the observations thus have to be reduced from the earth surface onto the geoid. This reduction is in geodetic literature called the *downward continuation.*

Correspondence to: P. Vaníček

The downward continuation may be applied to observed gravity values g, gravity disturbances δg, disturbing potential T, or any combination of these quantities. Once we know how to downward continue T, the downward continuation of the other quantities can be also derived. The main problem is that the space through which we want to reduce the desired quantity contains (topographical) masses with an irregular density distribution. It is relatively easy to downward continue a harmonic function, but it is very difficult to do so with a non-harmonic one since we would have to take into account the density of topographical masses. While T is harmonic outside the earth surface (disregarding the atmospheric density), it is certainly not harmonic within the topography.

The way this problem is usually treated is to transform it into a model space, where the disturbing potential to be dealt with is harmonic between the earth surface and the geoid. Two such models have been used in geodesy: the free-air model and the Helmert model. The former is employed in the context of solving the Molodenskij problem (Moritz, 1980) and it consists of "moving" topographical masses inside the geoid so as not to change the external potential. The downward continuation performed by means of this model thus constitutes the downward continuation of the external field T inside the topography (Vaníček and Martinec 1994). The latter model uses Helmert's "condensation" of topography onto the geoid by means of one of the condensation techniques, that may preserve either the total mass of the earth, or the location of the centre of mass, or to be just an integral mean of topographical column density – see, e.g., (Wichiencharoen 1982).

The open question in both these approaches is the existence of the harmonic downward continuation of the model field. In the free-air model, the model field coincides with the real field on the earth surface and as such is very complicated, because it is affected by the density irregularities in the close proximity of the earth surface, i.e., within the topography. It thus has constituents of all spatial frequencies with possibly large amplitudes. Yet, the physics the gravitational attraction in a region of harmonicity requires that constituents of different wave numbers n be suitably attenuated (by an approximate factor of $[(R+H)/R]^n$) when going from the geoid to the earth surface of height H above the

geoid. In other words, there probably does not exist a disturbing potential "corresponding to free-air anomaly" in the sense of eqn. (2), harmonic between the geoid and the earth surface, which would have the value T at the surface. This problem is usually overcome by some smoothing of T such as the Residual Terrain Model method (Forsberg 1984), called also "regularization", at the earth surface, the physical interpretation of which is unclear.

In the Helmert model, T is transformed to the Helmert disturbing potential T^h by the following equation

$$T^h = T - V, \tag{1}$$

where V is the difference between the potential of the topography and the potential of the Helmert condensation layer (Vaníček and Martinec 1994; Martinec and Vaníček, 1994). Helmert's disturbing potential at the earth surface is thus made smoother than the actual disturbing potential because the nearest "disturbing masses" are now located on the geoid. To illustrate this point, we show in Figure 1 a profile of free-air anomaly, defined to a spherical approximation as (Heiskanen and Moritz, 1967)

$$\Delta g_t^{fa} \doteq -\left.\frac{\partial T}{\partial r}\right|_t - \frac{2}{R} T_t, \tag{2}$$

at the earth surface t taken across a particularly rugged part of the Canadian Rocky Mountains and compare it with the same profile depicting the Helmert anomaly Vaníček and Martinec 1994)

$$\Delta g_t^{h} \doteq -\left.\frac{\partial T^h}{\partial r}\right|_t - \frac{2}{R} T_t^h, \tag{3}$$

given again to a spherical approximation. Even for the $5'$ step the smoothing effect of the "Helmertization" is already visible. The real difference would be seen at the high frequency part of the respective spectra, from wave number $n = 6,000$ onwards. The investigation of this difference is, however, not pertinent here.

The problem with the Helmertization of the disturbing potential is that the direct topographical effect V cannot be evaluated exactly; the density distribution within topography is not known very accurately and some density model has to be assumed. In the first approximation a constant topographical density of 2.67 g/cm^3 is normally used and this is the density model we have used in the experiment reported in this paper.

We note that eqn. (3) can be written also as (cf. eqn. (1))

$$\Delta g_t^{h} \doteq \Delta g_t^{fa} + \left.\frac{\partial V}{\partial r}\right|_t + \frac{2}{R} V_t, \tag{4}$$

where the second term on the right hand side is the *direct topographical effect* on gravity at the earth surface and the third term is called the *secondary indirect topographical effect* on gravity at the earth surface. They both are functions of topographical height H and topographical density ρ (Vaníček and Martinec, 1994) and can be evaluated numerically once a density model is assumed and a condensation technique adopted.

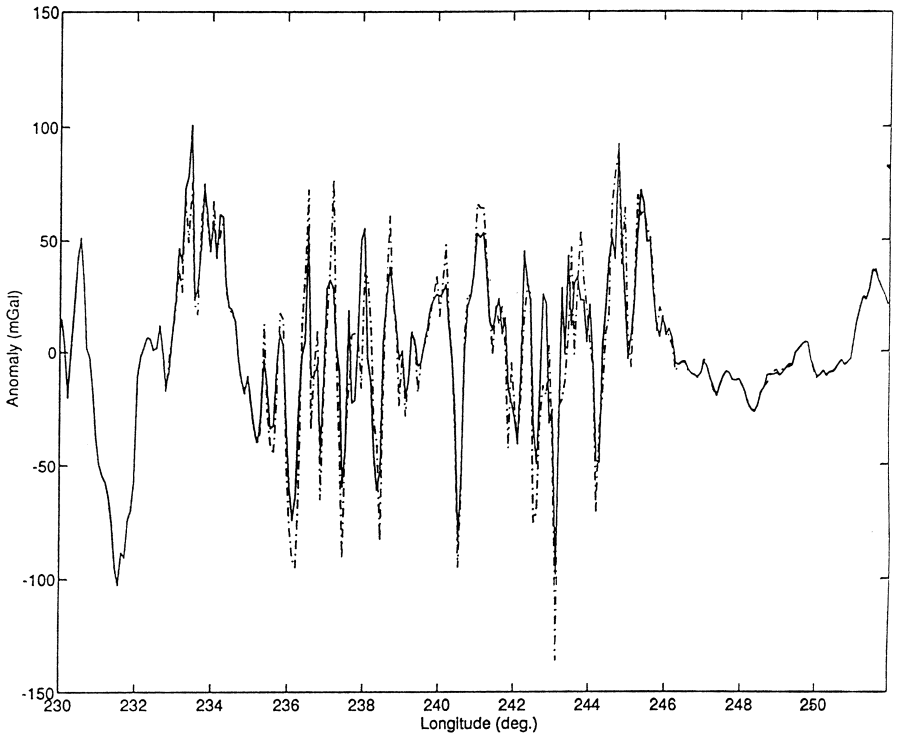

Fig. 1. Profile of free-air (– · – ·) and Helmert (–)$5' \times 5'$ gravity anomalies for latitude $\phi = 50°.417$

2. Application of Poisson's theorem

Let us now discuss the problem of "downward continuation" from the mathematical point of view. The standard mathematical apparatus used in studying downward as well as upward continuation is the Poisson theorem. The Poisson theorem states that from a function f, known on a sphere of radius R and harmonic outside this sphere, we can compute the functional value $f(r,\Omega)$ anywhere outside the sphere, i.e., for $r > R$ by the following (Poisson) integral (Kellogg 1929; MacMillan 1930)

$$f(r,\Omega) = \frac{1}{4\pi}\int_{\Omega'} f(R,\Omega')K(r,\psi,R)d\Omega', \tag{5}$$

where K is the Poisson's kernel

$$\begin{aligned} K(r,\psi,R) &= \sum_{j=0}^{\infty}(2j+1)\left(\frac{R}{r}\right)^{j+1}P_j(\cos\psi) \\ &= R\frac{r^2-R^2}{l^3}, \end{aligned} \tag{6}$$

ψ is the angular distance between geocentric directions Ω and Ω' and l is the spatial distance between (r,Ω) and (R,Ω'). This theorem can be directly applied to T^h, if we think the approximation of the geoid by the sphere of radius R is admissible; it guarantees an accuracy better than $1.3 * 10^{-3}$ which seems reasonable here.

An expression similar to (5) can be derived also for the radial derivative of a harmonic function f (Heiskanen and Moritz 1967)

$$\left.\frac{\partial f}{\partial r}\right|_{r,\Omega} = \frac{R}{4\pi r}\int_{\Omega'}\left.\frac{\partial f}{\partial r}\right|_{R,\Omega'}K(r,\psi,R)d\Omega'. \tag{7}$$

Again, to a spherical approximation of the geoid, this expression can be directly applied to the radial derivative of T^h. But the radial derivative of T^h is nothing else but *Helmert's gravity disturbance* (Heiskanen and Moritz 1967) δg^h and we can write for the unknown Helmert's gravity anomaly on the geoid (subscript g)

$$\begin{aligned} \Delta g_g^h &= \Delta g_t^h + \delta g_g^h - \delta g_t^h - \frac{2}{R}(T_g^h - T_t^h) \\ &= \Delta g_t^h - D\delta g^h - DT^h, \end{aligned} \tag{8}$$

where $D\delta_g^h$ is the downward continuation of Helmert's gravity disturbance called Dg^h in (Vaníček and Martinec 1994) and DT^h is the downward continuation of $2T^h/R$.

Denoting the difference $\Delta g_g^h - \Delta g_t^h$ by $D\Delta g^h$ and calling it the *downward continuation of Helmert gravity anomaly*, we can write eqn. (8) as

$$D\Delta g^h = -D\delta g^h - DT^h. \tag{9}$$

This equation shows that the only difference between the downward continuation of gravity disturbance and that of gravity anomaly is the term DT^h. This term

$$\begin{aligned} DT^h(\Omega) = &\frac{2}{R}T_g^h(\Omega) \\ &- \frac{1}{2\pi R}\int_{\Omega'} T_g^h(\Omega')K(r,\psi,R)d\Omega' \end{aligned} \tag{10}$$

is of a much lower spatial frequency than the $D\delta g^h$ term. For the degree n of the model equal to 180, the magnitude of T^h drops by two orders compared to Δg^h. It is also much smaller and can thus be adequately evaluated from a global model. This can be seen on the plot in Figure 2 showing the south-western corner of Canada that includes several chains of the Rocky Mountains.

3. Setting up the recursive formula

Since the (Helmert) gravity anomaly at the earth surface is more readily obtained than the (Helmert) gravity disturbance, we shall work with gravity anomalies rather than gravity disturbances.

From the Poisson integrals for T^h and $\partial T^h/\partial r$, and eqn. (3) we can easily derive the following expression

$$\begin{aligned} \Delta g_t^h &\doteq \frac{R}{4\pi r}\int_{\Omega'}\Delta g_g^h K(r,\psi,R)d\Omega' \\ &= I(\Delta g_g^h), \end{aligned} \tag{11}$$

good to the usual spherical approximation. The problem of downward continuation is then reduced to the solution of the above integral equation of first kind: Δg_t^h is known and Δg_g^h is to be determined.

Up to the sperical approximation, the integral equation (11) is valid exactly since T^h is harmonic above the geoid. Hence a unique solution Δg_g^h to eqn. (11) exists if T_g^h(on the geoid) is finite and Δg_t^h is exact. From the physics of the problem it should be obvious that indeed T_g^h is finite but it may have large amplitudes for short wavelength components. As the solution of our integral equation (of first kind) is inherently unstable, any errors in Δg_t^h may get amplified by the solution. Generally, the shorter wavelength errors will get amplified more than the longer wavelength ones. To aleviate this problem, we apply a stabilizing procedure consisting of using mean anomalies rather than point anomalies. (The application of Stokes's formula can be regarded as another stabilization process, of course) We shall return to this problem at the end of this section. First, we set up a simple recurrence process to solve the integral equation iteratively.

Let us begin by denoting

$$\Delta g_t^h - \mathbf{I}(\Delta g_g^h) = q; \tag{12}$$

clearly, according to eqn. (11), this difference equals to 0. We can define

$$q^{(k+1)} = \Delta g_t^h - \mathbf{I}\left[(\Delta g_g^h)^{(k)}\right], \tag{13}$$

where the superscript in brackets denotes the iteration number, and start the iterative process with

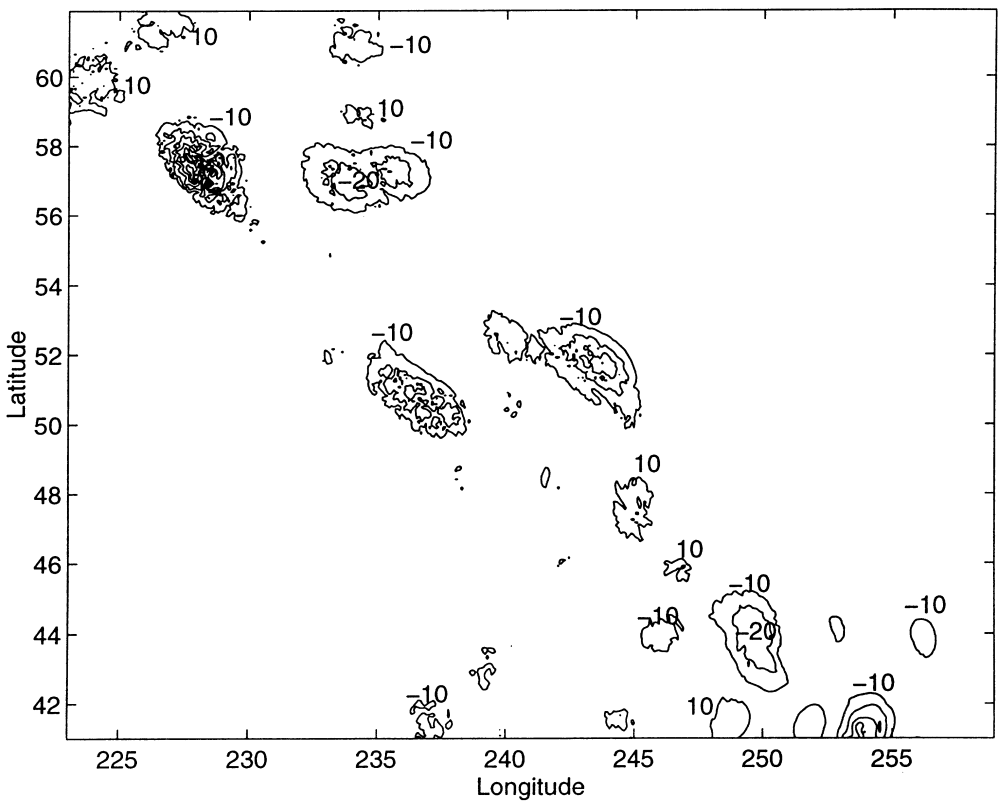

Fig 2. The downward continuation of $2T/R$ (μGal). Contour interval = 10 μGal

$$(\Delta g_g^h)^{(0)} = q^{(0)} = \Delta g_t^h. \tag{14}$$

We note that this implies

$$q^{(1)} = \Delta g_t^h - \mathbf{I}(\Delta g_t^h). \tag{15}$$

The sought quantity (Δg_t^h) is given by

$$\Delta g_g^h = \Delta g_t^h + \sum_{j=1}^{\infty} q^{(j)} = \sum_{j=0}^{\infty} q^{(j)} \tag{16}$$

and its iterative approximations are

$$(\Delta g_g^h)^{(k)} = \sum_{j=0}^{k} q^{(j)}. \tag{17}$$

The recursive formula for one point Ω then can be written as

$$\begin{aligned} q^{(k+1)}(\Omega) &= \Delta g_t^h(\Omega) - \frac{R}{4\pi r}\int_{\Omega'} \sum_{j=0}^{k} q^{(j)} K(r,\psi,R)\, d\Omega' \\ &= \Delta g_t^h(\Omega) - \mathbf{I}\left(\sum_{j=0}^{k} q^{(j)}\right). \end{aligned} \tag{18}$$

This equation can be easily converted to an operational recursive formula for the individual differences which reads

$$\begin{aligned} q^{(k+1)}(\Omega) &= q^{(k)}(\Omega) - \mathbf{I}(q^{(k)}) \\ &= q^{(k)}(\Omega) - \frac{R}{4\pi r}\int_{\Omega'} q^{(k)} K(r,\psi,R)\, d\Omega'. \end{aligned} \tag{19}$$

When we want to solve for the $\Delta g_g^h(\Omega)$ in a certain area A, we start the process by taking the known Helmert anomaly on the surface of the earth as the zeroth iteration (eqn. (14)) for all the points Ω in A and use eqn. (19) to compute the successive iterations, again, for all the points in A, till even the largest difference $q^{k+1}(\Omega)$ in A is in absolute value smaller than a prescribed limit. This limit can be set up to perhaps some 10μGal, which should ensure that the accuracy of geoid computed from so determined anomalies would not be affected above the magic 1cm level (Vaníček and Martinec 1994). Let us note here, that there exist better, i.e., faster converging schemes. A search for the best suited scheme was not considered necessary in this initial stage of our investigations. One such technique was pointed to us "after the fact" by Vermeer (1995, personal communication) and will be tested in subsequent investigations.

There are two problems with the process described above. The first one concerns the convergence of the iterative process – none of the discussion in this section gives us any hint as to the convergence of the process. This means that based on the discussion above, we cannot guarantee that the largest difference in A will ever be smaller than the prescribed limit. The potential non-convergence of the iterative process is related to the

above mentioned lack of stability of the solution. We will have more to say about it in sections 5 and 6.

The second problem is related to the integral appearing in eqn. (19) – this integral is to be taken over the whole earth and thus the differences $q^{(k+1)}(\Omega)$ have to be computed over the whole earth. We shall discuss the second problem in the next section.

4. Selecting integration limits

Fortunately, the Poisson kernel

$$K(r,\psi,R) = K(R+H,\psi,R) = K\left(\frac{H}{R},\psi\right) \tag{20}$$

that dominates the behaviour of the sub-integral function in eqn. (19), vanishes rather quickly with growing angular distance ψ – see Figure 3. This means that the integration in eqn. (19) can be taken only over a spherical cap of a relatively small radius ψ_0 (instead of over the whole earth) and the error committed by doing so – the integration truncation error which we will be calling here simply the *truncation error* – remains relatively small. This behaviour is governed by the height H of the point Ω: the higher the point, the slower the kernel vanishes.

We have tested different truncation radii ψ_0 for their truncation errors and determined that a truncation radius of 1° gives a reasonably small error for our test area in south-western Canada. Moreover, the truncation error can be reduced by introducing a modification of the Poisson kernel. The technique invented by Molodenskij, where the upper limit of the truncation error is minimized (Molodenskij et al. 1960; Sjöberg 1984; eqn. 13), appears to be well suited to our purpose. We shall now show, how this technique works in our context.

We begin by rewriting the integral in eqn. (19) as

$$\int_{\Omega'} q^{(k)} K(\Omega,\Omega')d\Omega' = \int_{C_0} q^{(k)} K(\Omega,\Omega')d\Omega' + \int_{\Omega'-C_0} q^{(k)} K(\Omega,\Omega')d\Omega', \tag{21}$$

where C_0 denotes the spherical cap of radius ψ_0. Clearly, the second term in eqn. (21) is the truncation error to be minimized and we shall denote it by Dg_T. The minimization is carried out in the sense of minimizing the upper bound of the absolute value of the truncation error (Vaníček and Sjöberg 1991 eqn. (15)) by subtracting from the Poisson's kernel an appropriately selected linear combination of spherical harmonic functions taken to a degree and order L. We have selected this upper limit to equal to 20. To be able to use the Molodenskij modification, we have to subtract first the low degree harmonics ($\leq L$) from the function to be convolved with the modified Poisson kernel. The low degree harmonics Δg_L have to be determined separately from a global gravity model and added to the truncation error Dg_T, which is also determined from a global gravity model. The determination of the appropriate coefficients of the modifying linear combination, some

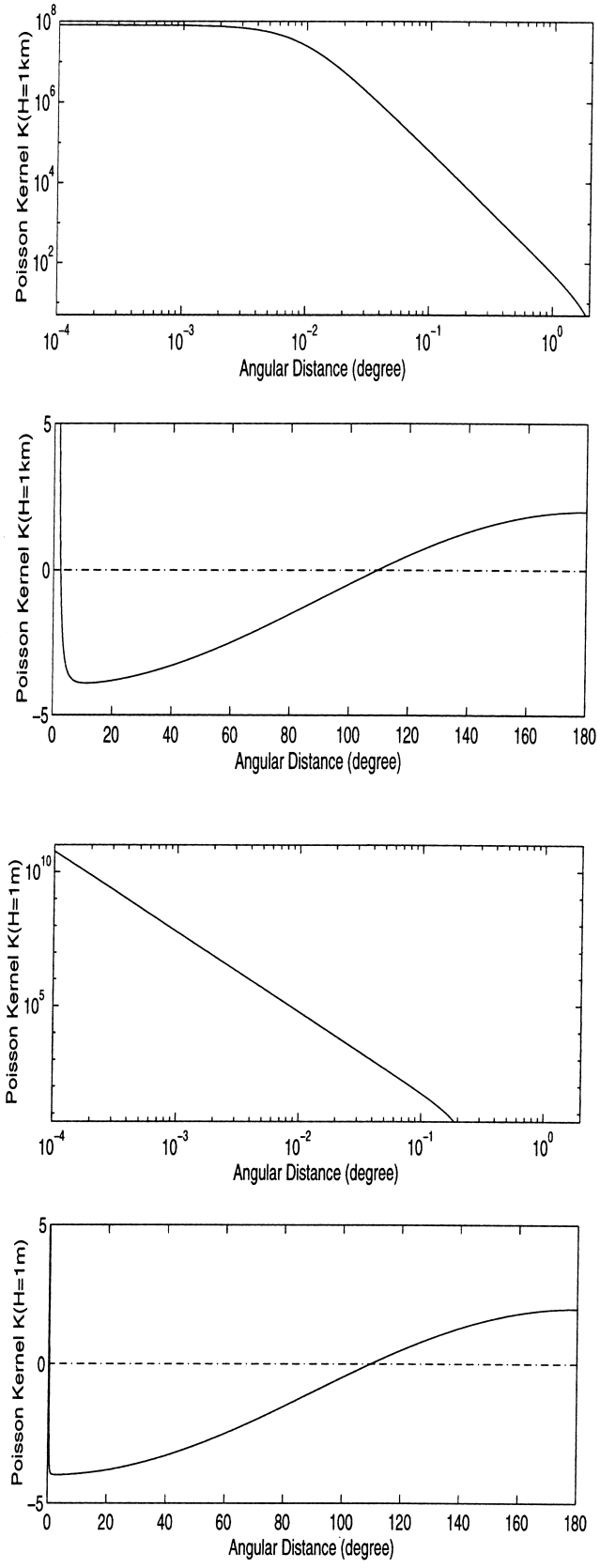

Fig. 3. Poisson's integration kernel for heights $H = 1,000$ m and $H = 1$ m. Note that the plots close to the computation point are in log. scale

properties of so modified Poisson's kernel, the derivation of the mathematical expression for the minimized truncation error and the expression for Δg_L are shown in the Appendix. Here, we just denote the so modified Poisson kernel by $K^m(\Omega, \Omega', \psi_0)$ and use it thus in our further derivations. Figure 4 illustrates what the modified Poisson kernel looks like so the interested reader can compare it with Figure 3. There is no discernible difference for $\psi < 1^\circ$.

The truncation error $Dg_T(\psi_0)$, which may still reach a few hundreds of μGal, has to be, of course, taken into account. But, the applicability of this approach is in that the truncation error changes only insignificantly from iteration to iteration and as such can be determined once for all in the first iterative step. This is particularly true in low terrain; in very high mountains the changes may be more significant and thus they may have to be taken under consideration, but this is unlikely. The correction for this error is then used in the iterations together with the correction Δg_L and the iterations are carried out only with the truncated Poisson integral. The truncation error Dg_T for our area of interest is plotted in Figure 5 (for GFZ93a global model, Gruber and Anzenhofer, 1993). The error in this area ranges from –0.14 mGal to 0.29 mGal.

5. Using mean Helmert's anomalies

Even after truncating the integration in eqn. (19) to a small spherical cap, we still have to integrate over each spherical cap, different for each point of interest and using the non-homogeneous modified Poisson kernel. This integration has to be done numerically, replacing the integration by summation over geographical cells of specified dimensions. The final product of our work, the Helmert anomaly on the geoid, is to be used in producing the geoid by Stokes's convolution integration, which is evaluated also by replacing the integration by a summation over (suitably weighted) mean anomalies on a grid of geographical cells (Heiskanen and Moritz 1967). It is thus natural, to use the same geographical grid for both tasks, i.e., to operate here with the same mean anomalies that we want to use in the Stokes convolution. In most applications these cells would be between 2.5′ by 2.5′ and 10′ by 10′. In Canada, we have been using 5′ by 5′ cells (Vaníček and Kleusberg 1987) and in our experiment here we use these as well.

We can now reformulate the equations derived above for the *mean Helmert anomalies*. We begin with eqn. (11) which we rewrite, for the mean anomaly in the i-th cell in the grid, as follows

$$\begin{aligned}\overline{\Delta g_t^h i} &= \frac{R}{4\pi r A_i}\int_{c_i}\int_{C_0} \Delta g_g^h(\Omega') K^m(r,\psi,R,\psi_0)\,d\Omega' d\Omega \\ &\quad + \overline{Dg_{1i}} \\ &= \frac{R}{4\pi r A_i}\int_{c_i}\int_{C_0} \Delta g_g^h(\Omega') K^m[H,\Omega,\Omega',\psi_0]\,d\Omega' d\Omega \\ &\quad + \overline{Dg_{1i}}, \end{aligned} \tag{22}$$

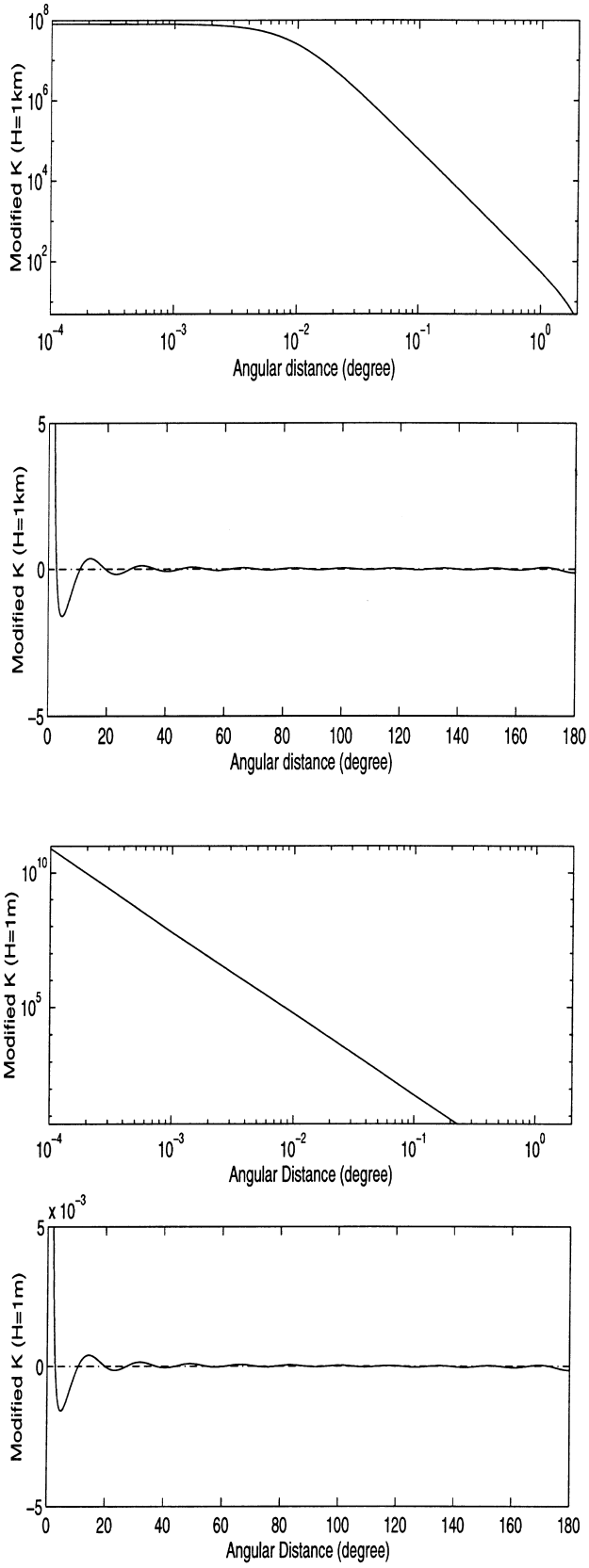

Fig. 4. Modified Poisson's integration kernel K^m for $H = 1,000$ m and $H = 1$ m

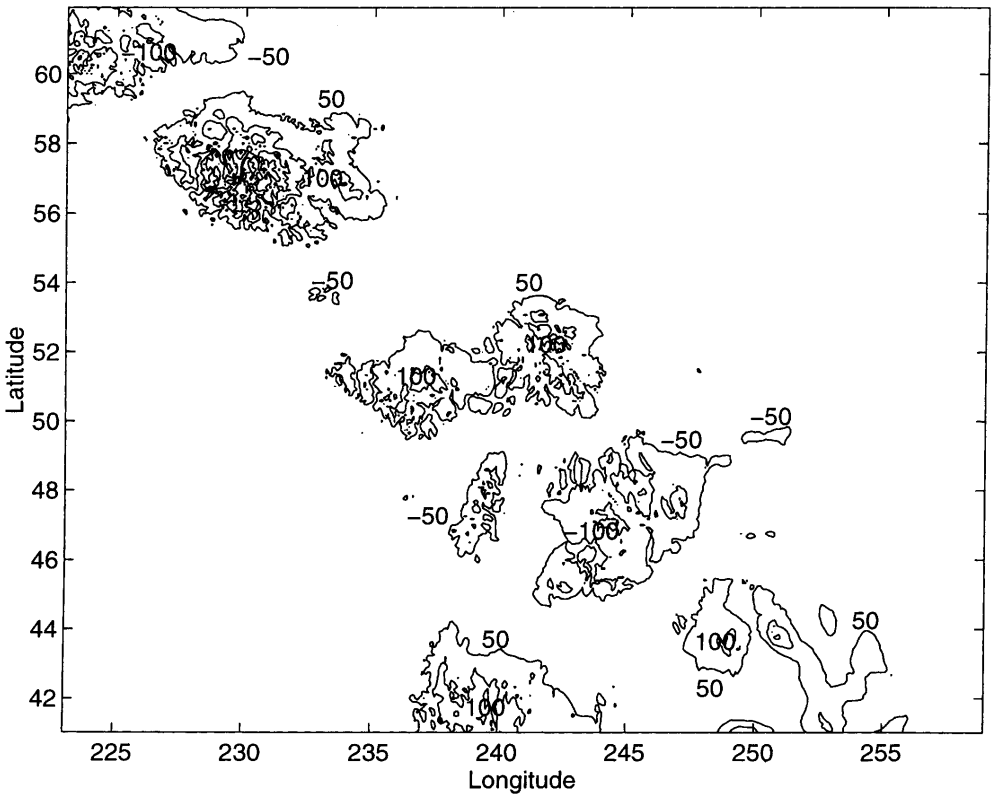

Fig. 5. Truncation error Dg_T (μGal). Contour interval = 50 μGal

where c_i denotes the i-th cell with area A_i and C_0 denotes again the spherical cap for the truncated integration. Note that since we use the modified Poisson kernel $K^m(H,\psi,\psi_0)$, the low frequency contribution is taken away automatically from the first term of eqn. (22). Then the second term $\overline{Dg_1}$ in eqn. (22) is the correction combining the low frequency contribution Dg_L and the truncation error Dg_T (see the Appendix for detail) averaged for the cell c_i. Interchanging the two integrations and denoting the mean value of the modified Poisson kernel by

$$\begin{aligned}\overline{K^m[H(\Omega_i),\Omega_i,\Omega']} &= \frac{1}{A_i}\int_{ci} K^m[H(\Omega),\Omega,\Omega',\psi_0]d\Omega \\ &= \overline{K_i^m(\Omega,\psi_0)},\end{aligned} \tag{23}$$

we get

$$\overline{\Delta g_t^h}_i = \frac{R}{4\pi r}\int_{C_0}\Delta g_g^h(\Omega')\overline{K_i^m(\Omega',\psi_0)}d\Omega' + \overline{Dg_{1i}}. \tag{24}$$

Expressing the integral over the cap as

$$\begin{aligned}&\int_{C_0}\Delta g_g^h(\Omega')\overline{K_i^m(\Omega',\psi_0)}d\Omega' \\ &\quad= \sum_j\int_{c_j}\Delta g_g^h(\Omega')\overline{K_i^m(\Omega',\psi_0)}d\Omega' \\ &\quad\doteq \sum_j\overline{\Delta g_g^h(\Omega_j')}\int_{cj}\overline{K_i^m(\Omega',\psi_0)d\Omega'} \\ &\quad= \sum_j\overline{(\Delta g_g^h)_j}\int_{cj}\overline{K_i^m(\Omega',\psi_0)}d\Omega' \\ &\quad= \sum_j\overline{(\Delta g_g^h)_j}\,\overline{\overline{K_{ij}^m}},\end{aligned} \tag{25}$$

where

$$\overline{\overline{K_{ij}^m}} = \frac{1}{A_i}\int_{ci}\int_{cj}K^m[H(\Omega_i),\Omega_i,\Omega']d\Omega'd\Omega, \tag{26}$$

is the doubly averaged modified Poisson kernel for the i-th and j-th cells and the summation is taken over all the cells contained within the integration cap of radius ψ_0. Then eqn. (22) can be rewritten as

$$\forall i:\ \overline{\Delta g_t^h}_i = \frac{R}{4\pi(R+H_i)}\sum_j\overline{\overline{K_{ij}^m}}\,\overline{\Delta g_{gj}^h} + \overline{Dg_{1_i}}, \tag{27}$$

which replaces the integral eqn. (11), valid for a point Ω, by a system of linear equations valid for all mean values of Helmert anomalies in the area of interest. It is this system of equations that has to be solved iteratively.

In order to get the recursive formulation that we need for the iterations, we simply replace the point Helmert anomalies in eqns. (12) to (15) by mean Helmert anomalies, ending up with the "mean difference" recurrence equation

$$\forall_i : \overline{q_i^{(k+1)}} = \overline{q_i^{(k)}} - \frac{R}{4\pi(R+H_i)} \sum_j \overline{\overline{K_{ij}^m}}\, \overline{q_j^{(k)}} \tag{28}$$

with the initial values

$$\forall_i : \overline{q_i^{(0)}} = \overline{\Delta g_{ti}^h} - \overline{Dg_{1i}} \ . \tag{29}$$

This is the final system that has to be iterated until all mean values $\overline{q}$ in A are in absolute value smaller than the prescribed limit. Note that both the gravity anomaly $\overline{\Delta g_{ti}^h}$ and the correction term $\overline{Dg_{1i}}$ (the sum of the truncation error and the low frequency contribution) only goes to the initial value (i.e., eqn. (29)), while for any k-th iteration $(k \neq 0), q^{(k)}$ can be obtained from the previous iteration $q^{(k-1)}$. The matrix of coefficients $\overline{\overline{K_{ij}^m}}$ is not symmetrical. It remains constant in the iterations and has a nice banded structure with the dominant elements residing on the main diagonal. For small H_i the i-th row is composed of small elements (that tend to zero when H_i goes to zero) and 4π on the main diagonal. This reflects the fact that for the height equals to zero, the downward continuation does not apply and the increments $q^{(k)}$ are, starting from $k = 1$ all equal to zero. As the height H_i grows larger, the off-diagonal elements grow larger and the Kronecker-like behaviour gets weaker and weaker.

We note, that the replacement of point Helmert anomalies by mean Helmert anomalies represents a further smoothing of the anomaly field. Thus working with mean Helmert anomalies increases the chances that the iterative process will indeed converge. Let us recall here that Bjerhammer (1962, 1976), in his famous formulation of the geodetic boundary value problem, proposed to carry out the downward continuation for point gravity anomalies. In Bjerhammar's approach, the additional smoothing by averaging over geographical cells employed here is absent.

Once all the individual "mean difference" $\overline{q_i^{(k)}}$ are calculated, we can obtain the final mean gravity anomalies $\overline{\Delta g_{gi}^h}$ and the mean downward continutaion of gravity anomalies $\overline{D\Delta g_i}$ as

$$\forall_i : \ \overline{\Delta g_{gi}^h} = \sum_{l=0}^{k} \overline{q_i^{(l)}} \tag{30}$$

$$\forall_i : \ \overline{D\Delta g_i} = \sum_{l=1}^{k} \overline{q_i^{(l)}} - \overline{Dg_{1i}} \ . \tag{31}$$

6. Results

In this section we report the results from our selected area (covering the southern part of the Canadian Rocky

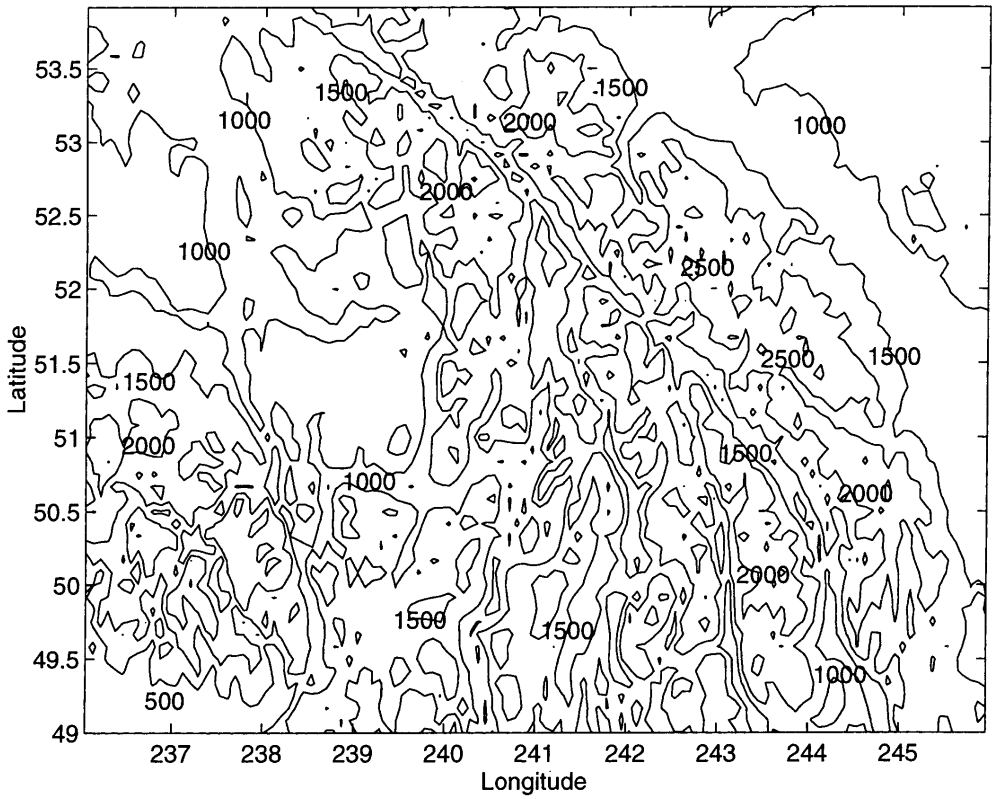

Fig. 6. Topographical heights in Canadian Rocky Mountains (m)

Mountains, see Figure 6), delimited by latitudes 49° N and 54° N, and longitudes 236° E and 246° E. The mean 5′ by 5′ heights in this area range between 0 and 2974 metres and the mean Helmert anomalies at the earth surface are between –134.17 mGal and 185.63 mGal. To reduce the effect of incomplete data coverage for integration caps (of 1° radius) along the edges of the area, we have increased the rectangular area by 6° in each direction so that the area for which the downward continuation is actually computed, is 17° by 22°, from which only 5° by 10° is used at the end.

We have investigated numerically the convergence of the iterative process in Tchebyshev's norm; the process converges, albeit fairly slowly. The iterations converge also in the quadratic norm, but this behaviour is only of an academic interest. In the 6° border area the solution is questionable, however, depending on the heights of the points outside the area of interest. (Experiments conducted after the submission of this manuscript have shown that the problematic border area is closer to 1°.) For instance, if all the points outside the extended area of interest have zero heights – think of an island at sea – the $q^{(1)}$ and all the higher iterations will be also equal to zero. In this case the errors made in the border area by integrating only over partial spherical caps would remain constant during the iterations and their effect would not spread into the internal rectangle. On the other hand, if points adjacent to the extended border have large heights, the errors from using partial integration areas (sections of the spherical caps) may be significant. This behaviour can be observed in the south-east corner of our area of interest.

In our inner rectangle of interest, the ratio of Tchebyshev norms, $\max|q^{k+1}|/\max|q^{(k)}|$, for any two successive iterations k-th and $(k+1)$st, is around 0.5. We note that for other points this ratio may be even larger than 1 but the number of points for which it is so decreases from iteration to iteration. Figure 7 shows the plot of $q^{(1)}$, while Figure 8 displays $q^{(10)}$, for the interested reader to compare the results for himself. The range of $q^{(1)}$ is < -42.13 mGal, 56.21 mGal $>$ and that of $q^{(10)}$ is < -2.71 mGal, 3.81 mGal $>$. In the course of these 9 iterations, the Tchebyshev norm decreases from 56.21 mGal to 3.81 mGal.

We have iterated the solution to $k = 45$, by which time the Tchebyshev norm had decreased to 0.01 mGal. We consider this sufficiently accurate even for accurate geoid computations. The solution was tested by back substitution, to make sure that accumulated round-off numerical errors did not affect the results beyond the required accuracy. The downward continuation of mean Helmert anomaly that we have been looking for, $\overline{D\Delta g^h}$, i.e., the sum of the increments $\overline{q^{(k)}}$ for k going from 1 to 45, is shown in Figure 9 for the internal rectangle of interest. The values are surprisingly large, comparable with the anomaly values themselves, but of predominantly short wavelength – it is thus impossible to display them graphically in a meaningful fashion. The 3-D display used here is not very useful but any other display mode is even worse. After getting the downward continuation, we finally obtain the Helmert's gravity anomaly on the geoid (see Figure 10). Since most of the power of $\overline{D\Delta g^h}$ is of a very short wavelength, however, the contribution to the Helmert co-geoid from this source is smaller than one would expect from the magnitude of the effect – see Figure 11. For our area of interest, it ranges between 0.096 and 1.096 metres.

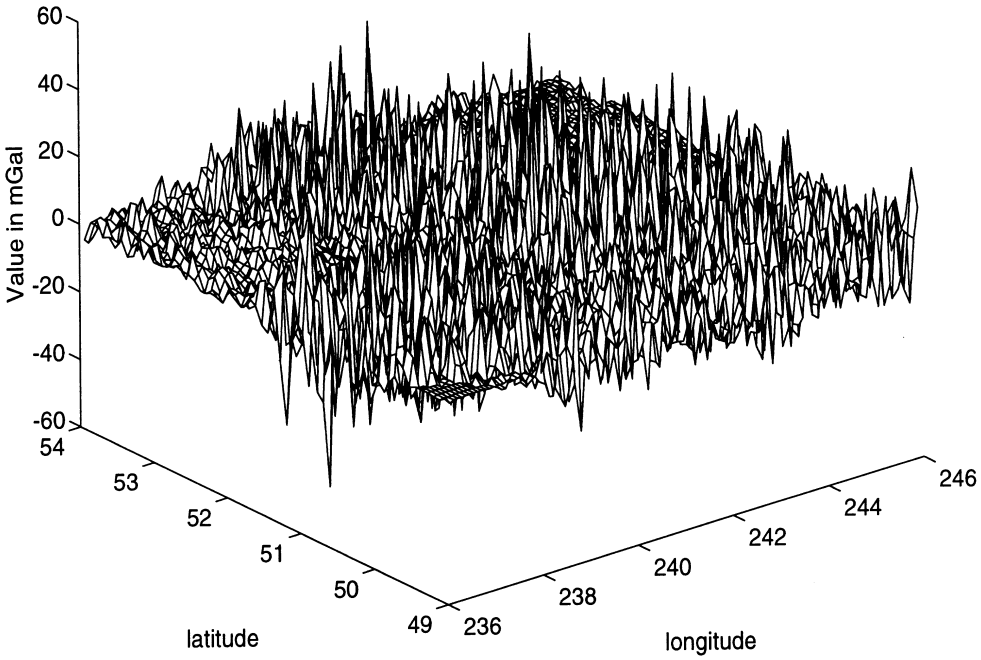

Fig. 7. First iteration $\overline{q^{(1)}}$ of $\overline{q}$ (mGal)

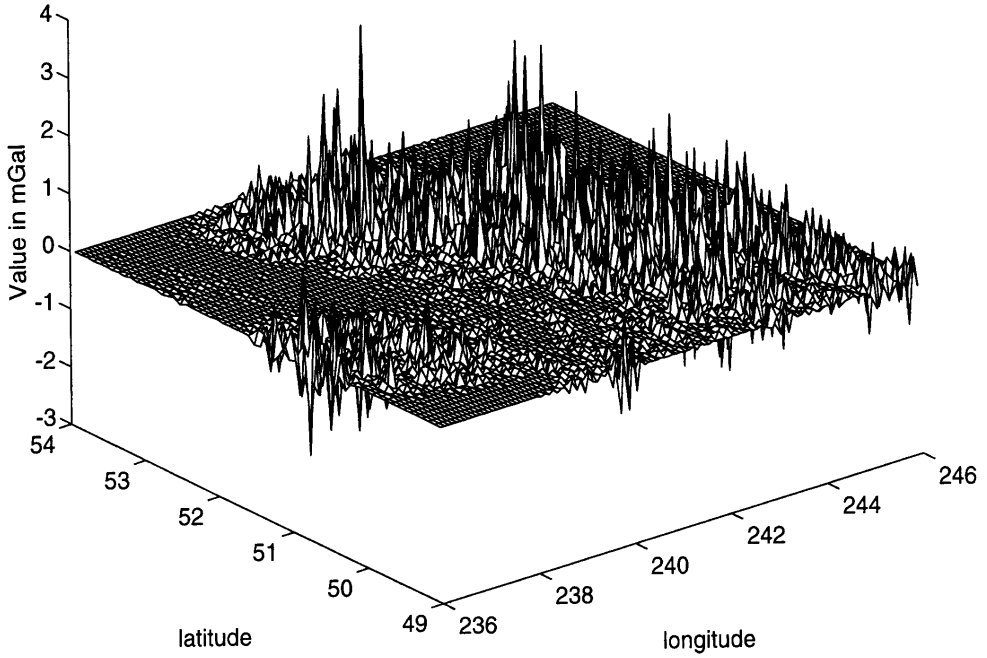

Fig. 8. Tenth iteration $\overline{q^{(10)}}$ of $\overline{q}$ (mGal)

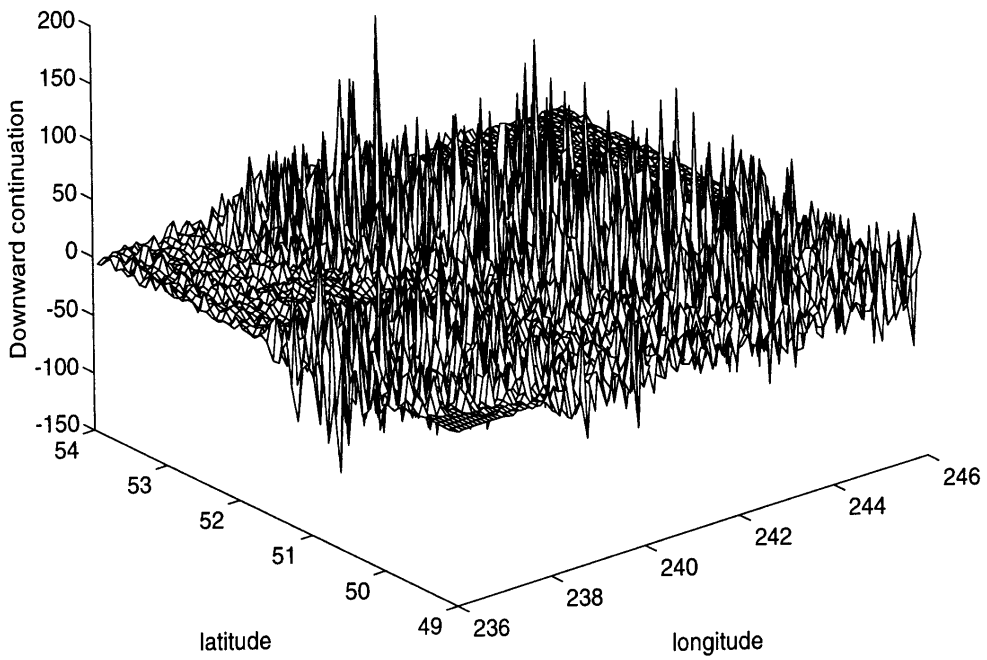

Fig. 9. Downward continuation $\overline{D\Delta_g}^h$ of $5' \times 5'$ mean Helmert's gravity anomalies (mGal)

7. Conclusions

We had set out to investigate a specific question as to whether mean Helmert's anomalies on the geoid can be derived from known mean Helmert's anomalies at the surface of the earth. In other words, we wanted to establish if the so called "downward continuation" of mean Helmert's anomalies can be computed or not. Our choice of *mean* anomalies was dictated by a practical consideration stemming from the realization that mean anomalies are the boundary values used in practice for solving the geodetic boundary value problem. Our choice of Helmert's anomalies came from the fact that: 1) Helmert's disturbing potential is harmonic outside the geoid and thus also between the geoid and the earth surface; 2) Helmert's gravity anomalies at the earth surface are by their nature smoother than the standard free-air anomalies. We had also decided to use mean anomalies for $5'$ by $5'$ geographical cells, because these were the ones we had readily at our disposal.

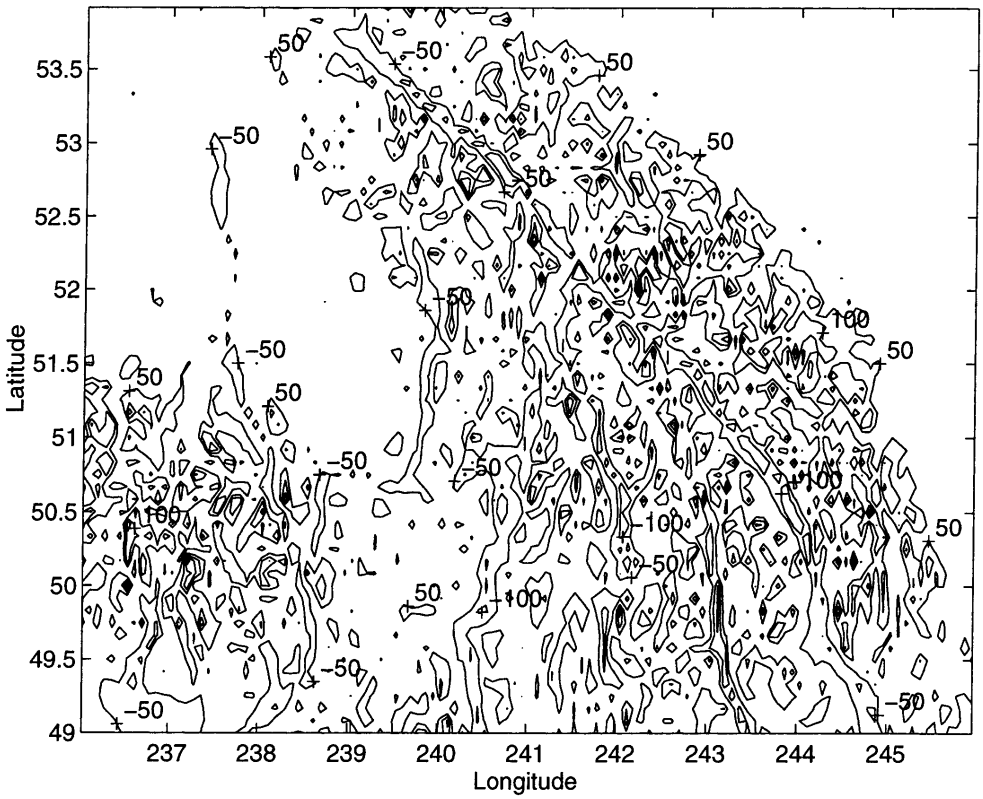

Fig. 10. Helmert mean gravity anomaly $\overline{(\Delta g_g^h)}$ on the geoid (mGal)

We have selected a particularly rugged part of Canada, the Rocky Mountains, in which to carry out our experiment. The reason for this choice should be obvious: if it turns out that the downward continuation can be computed in the Rockies, with mountains over 4,000 metres high, then there should be little trouble computing it anywhere else in the world, with perhaps the exception of the Himalayas.

When working with the Poisson problem, much like working with the Newton and Stokes problems, (i.e., the evaluation of the gravitational potential from Newton's integral and the evaluation of the geoid from Stokes's integral), one is supposed to evaluate a surface convolution integral over the whole earth, which is an impractical requirement. We have overcome this technical difficulty in much the same way as we overcome it in solving the other two problems, by splitting the integration area into a small spherical cap – we have chosen a cap of radius equal to 1 arc-degree – around the point of interest and the rest of the world. The contribution from the rest of the world is sufficiently small so that it can be evaluated to a sufficient accuracy using one of the existing global gravity models. To minimize this contribution further we also subtract the low degree and order field – to degree and order 20, has been our choice – from the observed mean Helmert's anomalies at the earth surface and downward continue this long wavelength part separately. Both these contributions (corrections) are evaluated in the spectral domain from the global model GFZ93a and added to the downward continuation of the higher degree and order – above 20 – mean Helmert's anomalies.

It turns out that the downward continuation of the higher degree and order mean Helmert's anomalies can be obtained in a fairly simple manner. For our 17° by 22° experimental area and the 5′ by 5′ mean anomalies, the Poisson integral equation is represented by 53,856 linear algebraic equations. We have evaluated the condition number for the corresponding matrix assembled for point values, rather than mean values. It is equal to 2, showing that the matrix is very well conditioned. (Our matrix, assembled for mean values, is probably somewhat less well conditioned, judging from the number of iterations needed.) There is thus no theoretical problem with getting the inverse of this matrix.

Because the size of the matrix is daunting, we had elected to solve the system by a simple iterative scheme. Table 1 shows how the iterations converge – to save space, only every 5th iteration is shown – in both Tchebyshev's and quadratic norms. It took 45 iterations to get the Tchebyshev norm under 10 μGal, i.e., to make sure that the downward continuation is accurate to at least 10 μGal for all the points in the area of interest. Interestingly, the quadratic norm of the iterated "mean differences" q decreases by almost 9 orders of magnitude in the course of the 45 iterations. Some 22 iterations would have sufficed if the mean threshold value of 10 μGal were used.

For physical reasons unknown to us the effect of the downward continuation of Helmert's anomalies (i.e., of

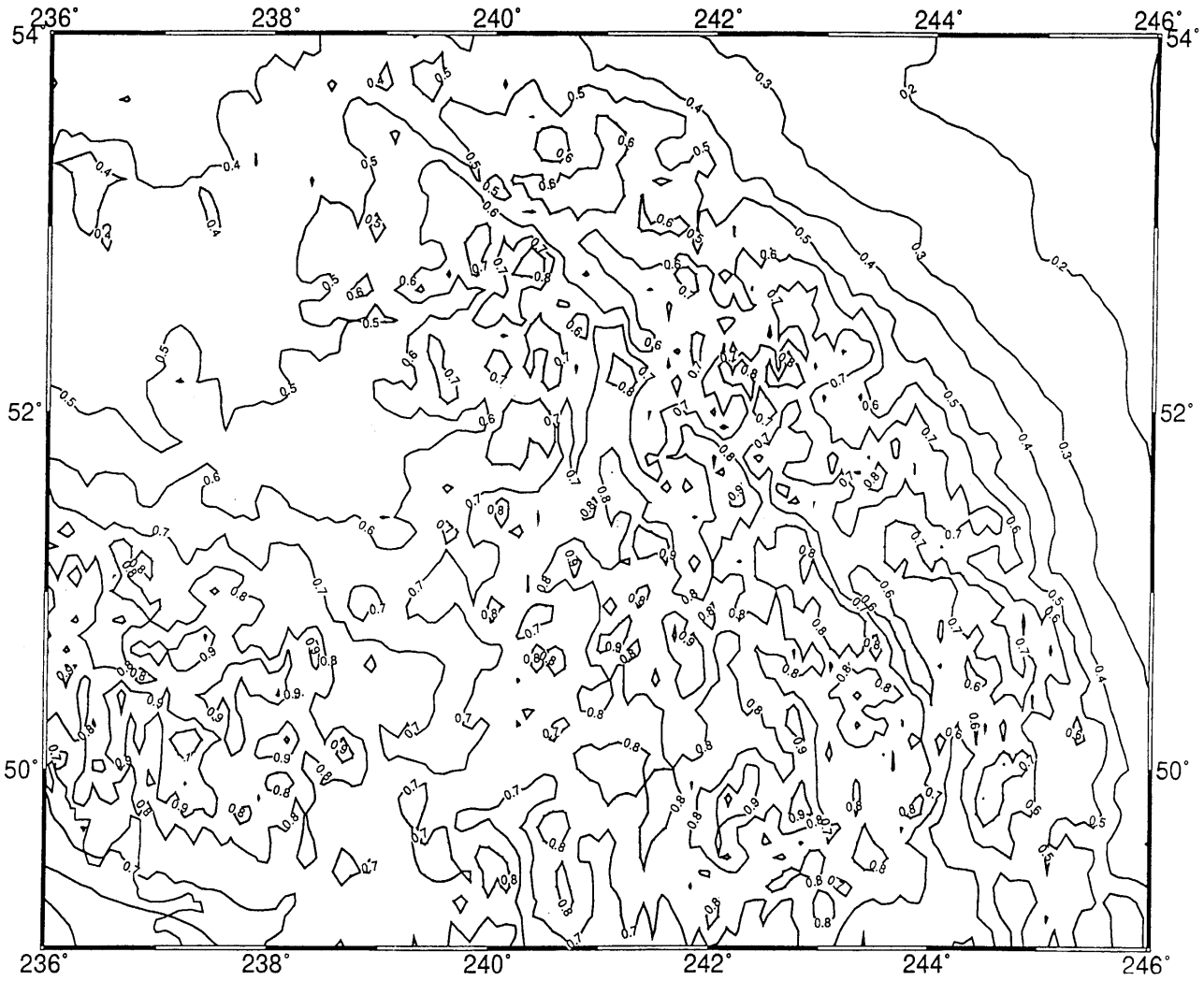

Fig. 11. Contribution to the Helmert co-geoid from the downward continuation of Helmert anomalies (m). Contour interval = 0.1 m

Table 1 Ranges and norms for every 5th iteration

n	Range of the effect $\sum_{i=1}^{n} q^{(i)}$ mGal	Tcheby. norm of $q^{(n)}$ mGal	quadratic norm of $q^{(n)}$ mGal^2
1	(− 42.13, 56.21)	56.21	0.2994E+2
5	(− 94.60, 146.05)	13.49	0.5457E+0
10	(−118.68, 179.23)	3.81	0.2598E−1
15	(−124.99 189.09)	1.17	0.2187E−2
20	(−126.79, 192.16)	0.44	0.2566E−3
25	(−127.32, 193.13)	0.20	0.3853E−4
30	(−127.49, 193.44)	0.10	0.7013E−5
35	(−127.55 193.54)	0.05	0.1477E−5
40	(−127.56, 193.58)	0.03	0.3448E−6
45	(−127.57, 193.59)	0.01	0.8619E−7

the difference between mean Helmert's anomalies on the earth surface and on the geoid) on Helmert's co-geoid (Vaníček and Martinec 1994) is everywhere positive – see Fig. 11. This is caused, mathematically, by the slight positive long wavelength bias of the downward continuation term. The high frequency variations of the downward continuation do not seem to have much of an effect on the co-geoid as Stokes's integration effectively dampens high frequency contributions.

We can thus claim that we have demonstrated that mean Helmert's anomalies can be successfully transferred from the surface of the earth to the geoid, i.e., that the downward continuation of mean Helmert's anomalies on a 5′ by 5′ grid is a well posed and therefore solvable problem. The natural smoothing (regularization) introduced by averaging the anomalies and the Poisson kernel over 5′ by 5′ (and possibly even much smaller) geographical cells is efficient enough to guarantee a unique solution of the downward continuation problem. Since in practical applications only mean anomalies rather than point anomalies are used, we believe that our results should put to rest the pervasive uneasiness about the solvability of the downward continuation problem. To be sure, there are still some theoretical questions to be worked out, such as: For what size of averaging cells will the solution show signs of breaking down, if at all? For what heights (averaged over the geographical cells) will the solution become unstable, if at all? Can a similar process be used for the

downward continuation of mean free-air anomalies encountered in Molodenskij's approach and under what circumstances? How good is the Pellinen approximation, which is normally used in the Molodenskij approach? But these questions are, of course, beyond the scope of this paper.

Acknowledgements. The research described in this contribution has been supported by an NSERC of Canada operating grant to the senior author and by a DSS contract with the Federal Government of Canada, Geodetic Survey Division (GSD) in Ottawa, let to the University of New Brunswick; we wish to thank Mr. M. Véronneau of the GSD for providing us with all the data used here. We wish to acknowledge that Dr. Martinec's stay in Canada, during the early stages of this research was supported by an NSERC grant for International Scientific Exchange, while Dr. Sun's presence on our team has been made possible by an NSERC International Fellowship grant. The senior author wishes to thank Dr. M. Vermeer for inspiring discussions conducted when he visited the Finnish Geodetic Institute earlier in 1994. Prof. Wm. R. Knight, UNB department of Mathematics and Statistics and department of Computer Science, gave us some useful hints for solving our large system of equations. Thorough reviews of the earlier versions of the manuscript by M. Vermeer and 2 anonymous reviewers led to a considerable improvement of the manuscript. The authors are truly grateful for the reviewers' effort.

Appendix: Low frequency contribution and truncation error

To estimate the truncation error of the downward continuation of gravity anomalies, we split the gravity anomaly on the geoid into two parts: low frequency part $(\Delta g_g^h)_L$ and high frequency part $(\Delta g_g^h)^L$:

$$\Delta g_g^h = (\Delta g_g^h)_L + (\Delta g_g^h)^L. \tag{32}$$

Eqn. (11) can then be written as

$$\begin{aligned}\Delta g_t^h &= \frac{R}{4\pi r}\int_{\Omega'} \Delta g_g^h K(r,\psi,R)d\Omega' \\ &= \Delta g_L + \frac{R}{4\pi r}\int_{\Omega'} (\Delta g_g^h)^L K(r,\psi,R)d\Omega',\end{aligned} \tag{33}$$

where

$$\Delta g_L = \frac{R}{4\pi r}\int_{\Omega'} (\Delta g_g^h)_L K(r,\psi,R)d\Omega' \tag{34}$$

is the low frequency part of gravity anomaly on the earth surface which can be calculated from a global gravity model. To transform eqn. (34) into spectral form, we use the following expression for gravity anomaly as obtained from a global Helmert's potential model T_{jm}^h

$$\Delta g_g^h(\Omega) = \gamma\sum_{j=2}^{\infty}(j-1)\sum_{m=-j}^{j} T_{jm}^h Y_{jm}(\Omega) \tag{35}$$

and the orthogonality relations

$$\frac{4\pi}{2j+1}\sum_{m=-j}^{j} Y_{jm}^*(\Omega')Y_{jm}(\Omega) = P_j(cos\psi), \tag{36}$$

$$\int_{\Omega} Y_{j_1m_1}^*(\Omega)Y_{j_2m_2}(\Omega)d\Omega = \delta_{j_1j_2}\delta_{m_1m_2}. \tag{37}$$

Since the first term on the right hand side of eqn. (32) can be obtained from eqn. (35) as

$$(\Delta g_g^h)_L = \gamma\sum_{j=2}^{L}(j-1)\sum_{m=-j}^{j} T_{jm}^h Y_{jm}(\Omega), \tag{38}$$

the low frequency contribution Δg_L becomes

$$\begin{aligned}\Delta g_L =& \frac{R\gamma}{4\pi r}\int_{\Omega'}\sum_{j_i=2}^{L}\sum_{m_1=-j_1}^{j_1}(j_1-1)T_{j_1m_1}^h Y_{j_1m_1}(\Omega') \\ &\times\sum_{j_2=0}^{\infty}(2j_2+1)\left(\frac{R}{r}\right)^{j_2+1} \\ &\times\frac{4\pi}{2j_2+1}\sum_{m_2=-j_2}^{j_2} Y_{j_2m_2}^*(\Omega')Y_{j_2m_2}(\Omega)d\Omega' \\ =&\gamma\sum_{j=2}^{L}(j-1)\left(\frac{R}{r}\right)^{j+2}\sum_{m=-j}^{j} T_{jm}^h Y_{jm}(\Omega).\end{aligned} \tag{39}$$

The integration in the second term on the right hand side of eqn. (33) can be truncated at spherical cap C_0 so that

$$\begin{aligned}&\frac{R}{4\pi r}\int_{\Omega'}(\Delta g_g^h)^L K(r,\psi,R)d\Omega' \\ &= +\frac{R}{4\pi r}\int_{C_0}(\Delta g_g^h)^L K^m(H,\psi,\psi_0)d\Omega' \\ &\quad+\frac{R}{4\pi r}\int_{\Omega'-C_0}(\Delta g_g^h)^L K^m(H,\psi,\psi_0)d\Omega' \\ &\quad+\frac{R}{4\pi r}\int_{\Omega'}(\Delta g_g^h)^L (K-K^m)d\Omega',\end{aligned} \tag{40}$$

where

$$\begin{aligned}K^m(H,\psi,\psi_0) =& K(H,\psi) \\ &-\sum_{j=0}^{L}\frac{2j+1}{2}t_j(H,\psi_0)P_j(\cos\psi)\end{aligned} \tag{41}$$

is the modified Poisson kernel with unknown coefficients t_j. The second term on the right hand side of eqn. (41) is the truncation error Dg_T to be minimized following the Molodenskij technique to minimize potential errors coming from the employed global model. The third term on the right hand side of eqn. (41) is equal to zero, because $(\Delta g_g^h)^L$ is the high frequency $(j > L)$ part of gravity anomaly and $(K - K^m)$ contains only the low frequencies $(j \le L)$. To get the unknown t_j's, we use Schwarz's inequality:

$$Dg_T^2 = \left(\frac{R}{4\pi r}\int_{\Omega'-C_0}(\Delta g_g^h)^L K^m(H,\psi,\psi_0)d\Omega'\right)^2$$
$$< \left(\frac{R}{4\pi r}\right)^2 \int_{\Omega'-C_0}[K^m(H,\psi,\psi_0)]^2 d\Omega'$$
$$\times \int_{\Omega'-C_0}[(\Delta g_g^h))^L]^2 d\Omega'. \quad (42)$$

To minimize the upper bound of $|Dg_T|$ we have to minimize $\int_{\Omega'-C_0}[K^m(H,\psi,\psi_0)]^2 d\Omega'$, i.e.,

$$\frac{\partial}{\partial t_j}\int_{\psi_0}^{\pi}\int_0^{2\pi}[K^m(H,\psi,\psi_0)]^2 \sin\psi d\psi d\alpha$$
$$= 2\pi\frac{\partial}{\partial t_j}\int_{\psi_0}^{\pi}[K^m(H,\psi,\psi_0)]^2 \sin\psi d\psi = 0. \quad (43)$$

Then the coefficients t_j can be obtained from the following system of equations:

$$\sum_{j=0}^{L}\frac{2j+1}{2}t_j(H,\psi_0)e_{ij}(\psi_0) = Q_i(H,\psi_0), \quad i = 0,1,\cdots,L, \quad (44)$$

where

$$e_{ij}(\psi_0) = \int_{\psi_0}^{\pi}P_i(\cos\psi)P_j(\cos\psi)\sin\psi d\psi,$$
$$Q_j(H,\psi_0) = \int_{\psi_0}^{\pi}K(H,\psi)P_j(\cos\psi)\sin\psi d\psi\,. \quad (45)$$

Writing the modified Poisson kernel in a spectral form

$$\overline{K^m}(H,\psi,\psi_0) = \sum_{j=0}^{\infty}\frac{2j+1}{2}\overline{Q}_j(H,\psi_0)P_j(\cos\psi), \quad (46)$$

where

$$\overline{Q}_j(H,\psi_0) = \int_{\psi_0}^{\pi}K^m(H,\psi,\psi_0)P_j(\cos\psi)\sin\psi d\psi, \quad (47)$$

we obtain the truncation error Dg_T as

$$Dg_T(\Omega) = \frac{R\gamma}{4\pi r}\int_{\Omega'}\sum_{j_1=2}^{\infty}\sum_{m_1=-j_1}^{j_1}(j_1-1)T_{j_1m_1}^h Y_{j_1m_1}(\Omega')$$
$$\times\sum_{j_2=0}^{\infty}\frac{2j_2+1}{2}\overline{Q}_{j_2}(H,\psi_0)$$
$$\times\frac{4\pi}{2j_2+1}\sum_{m_2=-j_2}^{j_2}Y_{j_2m_2}^*(\Omega')Y_{j_2m_2}(\Omega)d\Omega'$$
$$=\frac{R\gamma}{2r}\sum_{j=2}^{\infty}(j-1)\overline{Q}_j(H,\psi_0)$$
$$\times\sum_{m=-j}^{j}T_{jm}^h Y_{jm}(\Omega). \quad (48)$$

Finally, eqn. (33) can be rewritten as

$$\Delta g_t^h = \frac{R}{4\pi r}\int_{C_0}(\Delta g_g^h)^L K^m(H,\psi,\psi_0)d\Omega' + Dg_1, \quad (49)$$

where

$$Dg_1 = \Delta g_L + Dg_T \quad (50)$$

is the term to be used in eqns. (22)–(29) in the text. We note that it is only the higher frequency part of Δg_g^h, i.e., $(\Delta g_g^h)^L$, that is used in the solution of the Poisson integral equation.

References

Bjerhammar, A., 1962, Gravity reduction to a spherical surface, Report of the Royal Institute of Technology, Geodesy Division, Stockholm.

Bjerhammar, A., 1976, A Dirac approach to physical geodesy, Zeitschrift für Vermessungswesen, 101,41–44.

Forsberg, R., 1984, Gravity field terrain effect computations by FFT, Bull. Géod. 59, 342–360.

Gruber, T. and M. Anzenhofer, 1993, The GFZ 360 gravity field model, the European geoid determination, Proceedings of session G3, European Geophysical Society XVIII General Assembly, Wiesbaden, May 3–7, 1993, published by the geodetic division of KMS, Copenhagen. Eds. R. Forsberg and H. Denker.

Heiskanen, W.H., and H. Moritz, 1967, Physical Geodesy, W.H. Freeman and Co., San Francisco.

Kellogg, O.D. 1929, Foundations of Potential Theory. Springer, Berlin (reprinted 1967).

MacMillan, W.D., 1930, The Theory of the Potential. Dover reprint, 1958.

Martinec, Z. and P. Vaníček, 1994, Direct topographical effect of Helmert's condensation for a spherical approximation of the geoid, Manuscripta Geodaetica, 19, 257–268.

Molodenskij, M.S., V.F. Eremeev and M.I. Yurkina, 1960, Methods for Study of the External Gravitational Field and Figure of the Earth, English translation by Israel Programme for Scientific Translations, Jerusalem, for Office of Technical Services, Department of Commerce, Washington, D.C., 1962.

Moritz, H., 1980, Advanced Physical Geodesy, H. Wichmann Verlag, Karlsruhe.

Sjöberg, L.E., 1984, Least squares modification of Stokes' and Vening Meinesz' formulas by accounting for truncation and potential coefficient errors, Manuscripta Geodaetica, 9, 209–229.

Vaníček, P. and E.J. Krakiwsky, 1986, Geodesy: the concepts, (2nd corrected edition), North Holland, Amsterdam.

Vaníček, P. and A. Kleusberg, 1987, The Canadian geoid – Stokesian approach, Manuscripta Geodaetica, 12, 86–98.

Vaníček, P. and L.E. Sjöberg, 1991, Reformulation of Stokes's Theory for Higher than Second-Degree Reference Field and a Modification of Integration Kernels, JGR 96 (B4), 6529–6539.

Vaníček, P. and Z. Martinec, 1994, The Stokes-Helmert Scheme for the Evaluation of a Precise Geoid, Manuscripta Geodaetica, 19, 119–128.

Wichiencharoen, C., 1982, The indirect effects on the computation of geoid undulations, Department of Geodetic Science, Rep. #336, Ohio State University, Columbus, Ohio, USA.